

# Is the Rigidity of SARS-CoV-2 Spike Receptor-Binding Motif the Hallmark for Its Enhanced Infectivity? Insights from All-Atom Simulations

Angelo Spinello,<sup>#</sup> Andrea Saltalamacchia,<sup>#</sup> and Alessandra Magistrato<sup>\*</sup>



Cite This: *J. Phys. Chem. Lett.* 2020, 11, 4785–4790



Read Online

ACCESS |



Metrics & More

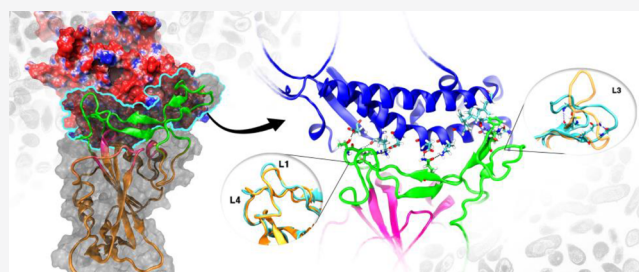


Article Recommendations



Supporting Information

**ABSTRACT:** The severe acute respiratory syndrome coronavirus (SARS-CoV-2) pandemic is setting the global health crisis of our time, causing a devastating societal and economic burden. An idiosyncratic trait of coronaviruses is the presence of spike glycoproteins on the viral envelope, which mediate the virus binding to specific host receptor, enabling its entry into the human cells. In spite of the high sequence identity of SARS-CoV-2 with its closely related SARS-CoV emerged in 2002, the atomic-level determinants underlining the molecular recognition of SARS-CoV-2 to the angiotensin-converting enzyme 2 (ACE2) receptor and, thus, the rapid virus spread into human body, remain unresolved. Here, multi-microsecond-long molecular dynamics simulations enabled us to unprecedentedly dissect the key molecular traits liable of the higher affinity/specificity of SARS-CoV-2 toward ACE2 as compared to SARS-CoV. This supplies a minute per-residue contact map underlining its stunningly high infectivity. Harnessing this knowledge is pivotal for urgently developing effective medical countermeasures to face the ongoing global health crisis.



The latest outbreak of a severe viral pneumonia, commonly referred as coronavirus disease 19 (COVID-19), originated in December 2019 in the city of Wuhan, China, has soon thereafter spread worldwide, being officially declared on March 11 a pandemic by the World Health Organization.<sup>1,2</sup> As of April 6th, COVID-19 had infected over 1.3 million patients and caused over 70 000 deaths worldwide. The pathogen responsible for this disease is a novel  $\beta$ -coronavirus ( $\beta$ -CoV) named severe acute respiratory syndrome coronavirus 2 (SARS-CoV-2) after its closely related SARS-CoV,<sup>3</sup> which, in 2002, caused 8096 cases and 774 deaths worldwide.<sup>4</sup> Additionally, a distinct coronavirus (Middle East respiratory syndrome coronavirus, MERS-CoV), in 2012, also spread in 27 different countries, causing 2494 cases and 858 deaths.<sup>5</sup> These numbers and the recurrence of this phenomenon underline that future outbreaks of new zoonotic threatening transmissions are likely to be expected in the future.

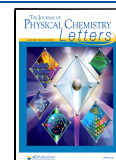
Similarly to other  $\beta$ -CoVs, the receptor-binding domain (RBD) of the homotrimeric viral spike (S) glycoprotein of SARS-CoVs mediates the molecular recognition to the host cellular receptor, acting as the Trojan horse for the virus entry into host cells. Hence, the S protein is considered a key molecular target for the design and development of specific antibodies<sup>6</sup> and is currently the object of burgeoning structural vaccinology studies. Stunningly, the phylogenetically similar S proteins of SARS-CoV and SARS-CoV-2 possess a sequence identity of about 77%,<sup>3</sup> both hijacking angiotensin-converting enzyme 2 (ACE2), a zinc metalloproteinase entailed with

cardiovascular and immune systems regulation,<sup>7,8</sup> to enter and infect human cells. The structural features of the interactions between the S protein and ACE2 are currently being addressed in many biophysical studies, aiming to clarify the reasons underlying the high human-to-human transmissibility of SARS-CoV-2 as compared to its closely related SARS-CoV variant. Cryo-EM and biophysical (surface plasmon resonance) studies provided insights on structure of the S glycoprotein's RBD in complex with ACE2, suggesting a higher binding affinity of SARS-CoV-2 toward ACE2 as compared to SARS-CoV.<sup>9,10</sup> This was corroborated by a cytometry analysis and immunofluorescence staining-based study.<sup>11</sup> Conversely, two distinct studies, based on biolayer interferometry, proposed that the RBD of the two SARS variants share a similar binding affinity toward ACE2.<sup>12,13</sup> In light of the ongoing global health emergency, this controversial evidence urgently calls for a rapid clarification. Aiming to extricate this puzzling scenario at the atomic level, we performed microsecond-long all-atom explicitly solvated molecular dynamics (MD) simulations of the RBD of SARS-CoV-2 and SARS-CoV/ACE2 adducts (Supplementary Movies S1 and S2), starting from their recently released structures (PDB IDs

Received: April 14, 2020

Accepted: May 28, 2020

Published: May 28, 2020



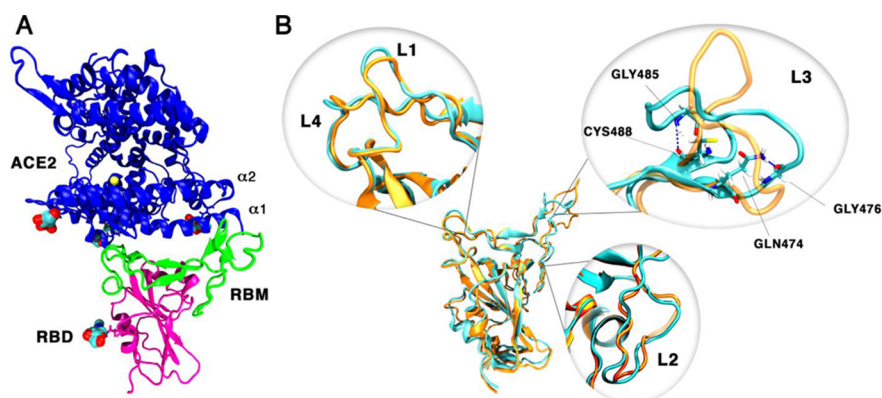


**Figure 1.** (A) Adduct between angiotensin-converting enzyme 2 (ACE2, blue) and RBD of SARS-CoV-2 (pink) with the RBM highlighted (green). Glycans and  $\text{Zn}^{2+}$  ions are depicted in van der Waals spheres and colored in cyan, red, and yellow for carbon, oxygen, and zinc atoms, respectively. (B) Alignment of the most representative structures of the RBD of SARS-CoV-2 (cyan) and SARS-CoV (orange), as obtained from a cluster analysis of the molecular dynamics trajectories. The insets compare the loops' (L1–2–3–4) structural organization.

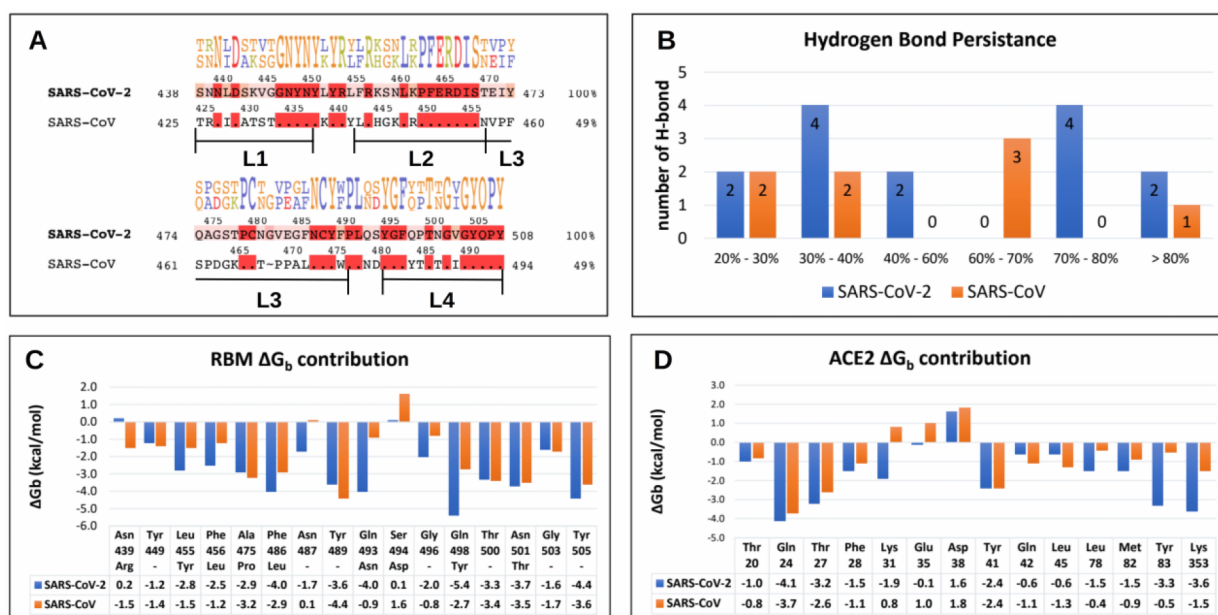


**Figure 2.** (A) Sequence alignment of SARS-CoV-2 and SARS-CoV RBM. Consensus residues are highlighted in red and shown with their letter code. A total sequence identity of 49% for the RBM is reported. (B) The number of H-bonds established at the two proteins' interface versus their persistence. Per-residue binding free energy ( $\Delta G_b$ , kcal/mol), calculated using the MM-GBSA method<sup>20</sup> of (C) the RBM and (D) ACE2.

6M0J and 6ACJ),<sup>14,15</sup> respectively (see Supporting Information for a detailed description). Most of the SARS-CoV(-2)'s residues binding to ACE2 belong to the RBD's receptor-binding motif (RBM, Figure 1A), which is made of four loops divided by two small  $\beta$ -strands.

During the MD simulations, the two SARS-CoV(-2)/ACE2 adducts establish stable interfacial interactions (Figure S1), showing structurally similar binding features. The main differences are restricted to a loop of the RBM (composed by Thr470-Pro491 and Asn457-Pro477 for SARS-CoV-2 and SARS-CoV, respectively, Figure 1B), which engages persistent interactions with ACE2. This recognition loop (hereafter also referred as loop 3, L3) is markedly more rigid in the SARS-CoV-2/ACE2 adduct as compared to its older variant (Figures S2 and S3). Indeed, L3@SARS-CoV-2 possesses a more defined secondary structure (composed by small  $\beta$ -sheets) that is preserved along the MD simulations (Figure S4). Ostensibly, L3's length is different in the two SARS variants, being

characterized by the insertion of Gly482 in SARS-CoV-2. This makes L3 longer and more structured, enabling it to gain stabilizing interactions (namely, the mutated residues Gly485 interacts with Cys488 and Gln474 with Gly476, Figure 1B) in the SARS-CoV-2/ACE2 adduct. This insertion, along with other amino acidic mutations (Figures 1B, 2A), converts a nonessential part of the RBM into an effective recognition grasp for ACE2, allowing SARS-CoV-2 to stiffen by establishing stronger interfacial interactions.

Indeed, the hydrogen (H-)bond analysis of the adducts pinpoints a larger number of more persistent H-bonds and salt bridges at the interface of SARS-CoV-2/ACE2 (Figure 2B and Table S1) as compared to its SARS predecessor. The residues establishing the most important H-bond interactions have been confirmed also in other simulation studies.<sup>16–19</sup>

This translates to a substantial difference of binding free energy ( $\Delta G_b$ ) between the two adducts, as obtained with a Molecular Mechanics Generalized Born Surface Area (MM-

GBSA) method, which favors SARS-CoV-2/ACE2 by 20.8 kcal/mol (Table S2), with the highest observed difference of 29.5 kcal/mol in the last part of the trajectory. Both the electrostatic and van der Waals components contribute to the enhanced  $\Delta G_b$ .<sup>20,21</sup> This remarkable difference in the  $\Delta\Delta G_b$  of SARS-CoV(-2)/ACE2 adducts is overestimated by the employed methodology, being nevertheless qualitatively consistent with the experimental  $K_d$  trend, which pinpoints a higher ACE2 binding affinity toward the novel coronavirus (15–44 and 185–326 nM for SARS-CoV-2 and SARS-CoV, respectively).<sup>9,10</sup>

Since a detailed atomic-level map of the key residues stabilizing the interactions of SARS-CoV-2 is pivotal for structure-based peptide design and vaccinology studies, we dissected the contribution (Figures 2C and D and Table S3) of each RBM's residue to the  $\Delta G_b$ . Remarkably, most of the residues differing in the RBM of the two SARS-CoV variants (i.e., Leu455/Tyr442, Phe456/Leu443, Gln493/Asn479, and Gln498/Tyr484 in SARS-CoV-2/SARS-CoV, respectively) contribute to increasing the binding affinity (i.e., decrease the  $\Delta G_b$ ) of the SARS-CoV-2/ACE2 adduct. As an example, Gln498@SARS-CoV-2 (Tyr484@SARS-CoV) strongly H-bonds with Lys353@ACE2 and Asp38@ACE2- $\alpha 1$ , resulting in a  $\Delta G_b$  gain of  $-4.8$  kcal/mol (Figures 2C and D, Figure 3). A

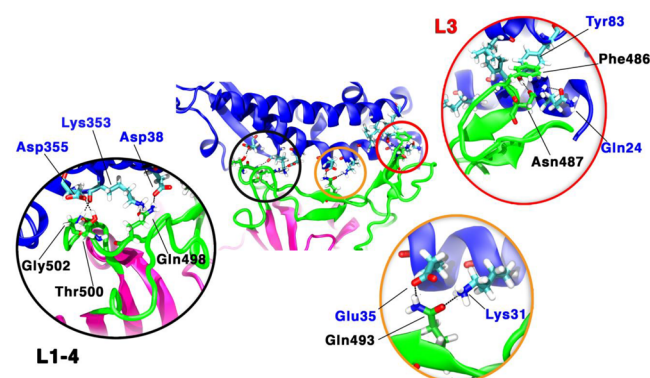


**Figure 3.** Key residues engaging hydrogen bonds and  $\pi$ -stacking interactions at the SARS-CoV-2/ACE2 interface (blue and green ribbons, respectively), as evidenced by MD simulation trajectory. Hydrogen bonds are highlighted as black dashed lines.

local reshaping of the interfacial H-bonds enables even the conserved residues to intertwine a stronger network of interactions with the receptor. Namely, the conserved Asn487@SARS-CoV-2 (Asn473@SARS-CoV) on L3 gives a larger contribution to  $\Delta G_b$  in the SARS-CoV-2/ACE2 adduct by H-bonding with Tyr83@ACE2- $\alpha 2$  (persistence 80.7%, Figure 3 and Table S1). Due to the higher L3 flexibility in the SARS-CoV/ACE2 adduct (Figure S2), this H-bond is lost, inducing a  $\Delta G_b$  decrease of 4 kcal/mol.

This detailed per-residue topological signature of the binding interface also discloses that Asp480@SARS-CoV has a negative impact on  $\Delta G_b$ . This residue forms only a low-persistent salt-bridge with Lys439@SARS-CoV which, due to RBM's flexibility, breaks for most of the MD trajectory. Thus, because Asp480 destabilizes the SARS-CoV/ACE2 adduct owing to the electrostatic repulsion with two nearby negatively charged residues (Glu35 and Asp38@ACE2- $\alpha 1$ , Figures 2C and D), the mutation to Ser494@SARS-CoV-2 resolves this unfavorable contribution.

Finally, a comparison of the electrostatic potential at the ACE2's interface with the two SARS variants did not reveal marked differences. In particular, SARS-CoV-2 showed only a slightly wider negatively charged surface (Figure S5).

To better decrypt the relative importance of the distinct components of RBM, we computed the Pearson-based cross-correlation matrix (CCM) of both SARS-CoV(-2)/ACE2 adducts, capturing the dynamically coupled motions and pinpointing dynamical differences between the two  $\beta$ -CoV variants.<sup>22</sup> Although by comparing the two matrices no difference has been detected on the ACE2's dynamics (Figure S6), by focusing on the interfacial residues, some diversities appear. Strikingly, all the RBM's loops besides L2, which is the farthest from ACE2, exhibit an increased correlation in SARS-CoV-2/ACE2 (Figure 4) as compared to SARS-CoV/ACE2 adduct. This is particularly true for L3, whose increased content of secondary structure (Figure S4) affects the strength of the interactions, and in turn the positive correlations, with the residues of the two interfacial ACE2's  $\alpha$ -helices (residues 19–45@ACE2- $\alpha 1$  and 79–83@ACE2- $\alpha 2$ , respectively). As well, L1 and L4 increase the grip to ACE2, gaining correlations with its nearby residues (324–330, 351–357, 386–393).

By summing the per-residue correlations of these matrices (i.e., measuring the per-residue correlation significance), we pinpoint the cardinal RBM's residues for ACE2 recognition (Table S3). Among these, the atomic fluctuations of Asn501@SARS-CoV-2 have a striking impact on the surrounding interactions, being at the center of an intricate H-bonding network. Because of its intermolecular H-bond with Gln498@SARS-CoV-2, Asn501 enables it to firmly interact with Asp38@ACE2- $\alpha 1$  and Lys353@ACE2. Remarkably, this analysis pinpoints the relevance of another mutated residue located on L3, i.e. Phe486@SARS-CoV-2, as compared to Leu472@SARS-CoV, which performs  $\pi$ -stacking interaction with Tyr83@ACE2- $\alpha 2$  (Figure 3), contributing to L3 stabilization and thus to ACE2 recognition.

Our results support and expand the first attempts to capture the key interactions of the SARS-CoV-2/ACE2 complex performed at structural and bioinformatics levels,<sup>23,24</sup> predicting the importance of critical residues (i.e., Gln498 and Phe486 mutations in SARS-CoV-2). The so-far available experimental structures of the SARS-CoV-2(RBD)/ACE2<sup>15,25</sup> supplied precious information on their interfacial H-bond network. Nevertheless, these structural studies can provide only a static picture, being unable to exhaustively unravel the relative importance of these key interfacial interactions. Our finite temperature all-atom simulations complement these pieces of information, uncovering the relative strengths and persistence of the principal interactions engaged by key mutations occurring in SARS-CoV-2 (Table S4). As a result, the critical chemical determinants for the higher stability of the SARS-CoV-2/ACE2 adduct. Additionally, our MD simulations disclose an induced fit of the ACE2- $\alpha 1$  helix which, along the MD trajectory, better adapts to the RBD@SARS-CoV-2 by increasing its tilt (Figure S7).

Owing to its extremely high contagiousness, the COVID-19 pandemic is dramatically hitting every country one by one while taking an increasingly deadly toll of lives. Because no therapeutic options are available for COVID-19, identifying effective medical countermeasures is a current global clinical urgency. Despite the high sequence identity between SARS-CoV and SARS-CoV-2, potent neutralizing antibodies specific for targeting ACE2's binding site of SARS-CoV/ACE2 (Figure

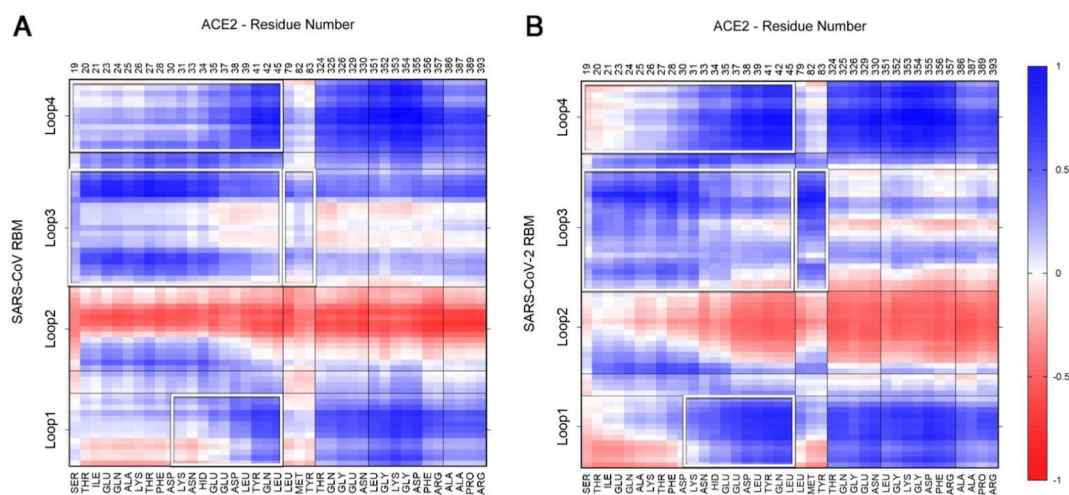


**Figure 4.** Cross-correlation matrix of the residues at the interface between ACE2 and (A) SARS-CoV and (B) SARS-CoV-2, based on per-residue Pearson's correlation coefficients (CCs) as derived from the mass-weighted covariance matrix calculated over 800 ns of molecular dynamics simulation trajectory. CC values range from  $-1$  (red, anticorrelated motions) to  $+1$  (blue, correlated motions). RBM is separated into loops. ACE2 residues are divided according to their secondary structure element. ACE2's residue names and numbers are listed on the bottom and top of the matrix, respectively. White squares pinpoint the regions with the largest differences.

5A),<sup>29,30</sup> failed to bind SARS-CoV-2 spike protein.<sup>9,13</sup> Remarkably, the crystal structure of the CR3022 antibody,

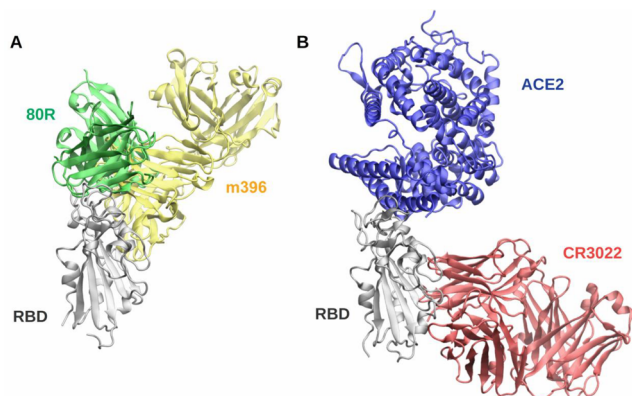


**Figure 5.** (A) Superposition of the adducts between the RBD of SARS-CoV (silver ribbons) and the antibody 80R (PDB code: 2GHW, green)<sup>26</sup> and m396 (PDB code: 2DD8, yellow).<sup>27</sup> (B) Structure of the CR3022/SARS-CoV-2/ACE2 ternary adduct obtained from an alignment of the crystal structure between CR3022 (red) and the RBD of SARS-CoV-2 (PDB code: 6W41)<sup>28</sup> and the structure of the most representative cluster as obtained from our molecular dynamics trajectories, highlighting the use of different epitopes for their binding.

isolated from a convalescent SARS patient,<sup>31</sup> disclosed a cryptic epitope on the S protein of SARS-CoV-2 (Figure 5B),<sup>28</sup> for which no competition with ACE2 is required. This suggests that this virus has a complex interactome to unravel and exploit for vaccine and drug design studies. In this context, the structural and dynamical differences recorded at the interfaces of the SARS-CoV(-2)/ACE2 adducts and the higher  $\Delta G_b$  of SARS-CoV-2 toward ACE2 provide a rationale to this lack of cross-reactivity, fostering the identification of novel epitopes as exclusive and specific hallmarks of SARS-CoV-2.

In conclusion, our outcomes unprecedentedly disclose the key molecular traits underlying the higher affinity of SARS-CoV-2 toward the human host ACE2 receptor, supplying a meticulous atomic-level topological map of the critical residues and the

pivotal interactions triggering SARS-CoV-2's entrance into the host cells. The very first step of SARS viral infection is, indeed, the ACE2 receptor recognition by the S protein. Hence, the enhanced binding affinity of SARS-CoV-2 toward ACE2, as compared to that of SARS-CoV, disclosed by us and by recent experimental studies,<sup>9,11</sup> is most likely correlated with its remarkable human-to-human transmissibility.<sup>12,32</sup> Besides rationalizing the high infectivity of SARS-CoV-2, our study provides novel fundamental advances for boosting the urgent development of effective therapeutic strategies such as peptide or antibody design, able to exploit and optimize the identified interactions. Moreover, with SARS-CoV-2 being highly specific toward its receptor, even compared with the closely related angiotensin-converting enzyme (ACE, Figure S8), ACE2 may also represent a new target for the development of antivirals as a potential strategy for new COVID-19 treatment. This information will contribute to facing the ongoing COVID-19 pandemic and possibly to fighting future coronavirus outbreaks.

## ■ ASSOCIATED CONTENT

### Supporting Information

The Supporting Information is available free of charge at <https://pubs.acs.org/doi/10.1021/acs.jpcllett.0c01148>.

Computational details, Figures S1–S8, and Tables S1–S4 (PDF)

Movie S1 shows the key interacting residues, during our molecular dynamics simulations, of the SARS-CoV-2/ACE2 adducts (AVI)

Movie S2 shows the key interacting residues, during our molecular dynamics simulations, of the SARS-CoV/ACE2 adducts (AVI)

## ■ AUTHOR INFORMATION

### Corresponding Author

Alessandra Magistrato – CNR-IOM c/o SISSA, 34136 Trieste, Italy; [orcid.org/0000-0002-2003-1985](https://orcid.org/0000-0002-2003-1985); Email: [alessandra.magistrato@sissa.it](mailto:alessandra.magistrato@sissa.it)

## Authors

Angelo Spinello – CNR-IOM c/o SISSA, 34136 Trieste, Italy;  
orcid.org/0000-0002-8387-8956

Andrea Saltalamacchia – International School for Advanced Studies SISSA, 34136 Trieste, Italy; orcid.org/0000-0003-1174-9271

Complete contact information is available at:

<https://pubs.acs.org/10.1021/acs.jpcllett.0c01148>

## Author Contributions

#A. Spinello and A. Saltalamacchia contributed equally to this work.

## Notes

The authors declare no competing financial interest.

## ACKNOWLEDGMENTS

A. Spinello was supported by a FIRC-AIRC “Mario e Valeria Rindi” fellowship for Italy. A.M. is thankful for the financial support of the project “Finding personalized therapies with in silico and in vitro strategies” (ARES) CUP: D93D19000020007 POR FESR 2014 2020-1.3.b, Friuli Venezia Giulia.

## REFERENCES

- Huang, C.; Wang, Y.; Li, X.; Ren, L.; Zhao, J.; Hu, Y.; Zhang, L.; Fan, G.; Xu, J.; Gu, X.; Cheng, Z.; Yu, T.; Xia, J.; Wei, Y.; Wu, W.; Xie, X.; Yin, W.; Li, H.; Liu, M.; Xiao, Y.; Gao, H.; Guo, L.; Xie, J.; Wang, G.; Jiang, R.; Gao, Z.; Jin, Q.; Wang, J.; Cao, B. Clinical features of patients infected with 2019 novel coronavirus in Wuhan. *Lancet* **2020**, *395* (10223), 497–506.
- Chan, J. F.; Yuan, S.; Kok, K. H.; To, K. K.; Chu, H.; Yang, J.; Xing, F.; Liu, J.; Yip, C. C.; Poon, R. W.; Tsoi, H. W.; Lo, S. K.; Chan, K. H.; Poon, V. K.; Chan, W. M.; Ip, J. D.; Cai, J. P.; Cheng, V. C.; Chen, H.; Hui, C. K.; Yuen, K. Y. A familial cluster of pneumonia associated with the 2019 novel coronavirus indicating person-to-person transmission: a study of a family cluster. *Lancet* **2020**, *395* (10223), 514–523.
- Zhou, P.; Yang, X. L.; Wang, X. G.; Hu, B.; Zhang, L.; Zhang, W.; Si, H. R.; Zhu, Y.; Li, B.; Huang, C. L.; Chen, H. D.; Chen, J.; Luo, Y.; Guo, H.; Jiang, R. D.; Liu, M. Q.; Chen, Y.; Shen, X. R.; Wang, X.; Zheng, X. S.; Zhao, K.; Chen, Q. J.; Deng, F.; Liu, L. L.; Yan, B.; Zhan, F. X.; Wang, Y. Y.; Xiao, G. F.; Shi, Z. L. A pneumonia outbreak associated with a new coronavirus of probable bat origin. *Nature* **2020**, *579* (7798), 270–273.
- de Wit, E.; van Doremalen, N.; Falzarano, D.; Munster, V. J. SARS and MERS: recent insights into emerging coronaviruses. *Nat. Rev. Microbiol.* **2016**, *14* (8), 523–34.
- Zaki, A. M.; van Boheemen, S.; Bestebroer, T. M.; Osterhaus, A. D.; Fouchier, R. A. Isolation of a novel coronavirus from a man with pneumonia in Saudi Arabia. *N. Engl. J. Med.* **2012**, *367* (19), 1814–20.
- Du, L.; He, Y.; Zhou, Y.; Liu, S.; Zheng, B. J.; Jiang, S. The spike protein of SARS-CoV-a target for vaccine and therapeutic development. *Nat. Rev. Microbiol.* **2009**, *7* (3), 226–36.
- Turner, A. J.; Hiscox, J. A.; Hooper, N. M. ACE2: from vasopeptidase to SARS virus receptor. *Trends Pharmacol. Sci.* **2004**, *25* (6), 291–4.
- Hoffmann, M.; Kleine-Weber, H.; Schroeder, S.; Kruger, N.; Herrler, T.; Erichsen, S.; Schiergens, T. S.; Herrler, G.; Wu, N. H.; Nitsche, A.; Muller, M. A.; Drosten, C.; Pohlmann, S. SARS-CoV-2 Cell Entry Depends on ACE2 and TMPRSS2 and Is Blocked by a Clinically Proven Protease Inhibitor. *Cell* **2020**, *181*, 271.
- Wrapp, D.; Wang, N.; Corbett, K. S.; Goldsmith, J. A.; Hsieh, C. L.; Abiona, O.; Graham, B. S.; McLellan, J. S. Cryo-EM structure of the 2019-nCoV spike in the prefusion conformation. *Science* **2020**, *367* (6483), 1260–1263.
- Shang, J.; Ye, G.; Shi, K.; Wan, Y.; Luo, C.; Aihara, H.; Geng, Q.; Auerbach, A.; Li, F. Structural basis of receptor recognition by SARS-CoV-2. *Nature* **2020**, *581*, 221.
- Tai, W.; He, L.; Zhang, X.; Pu, J.; Voronin, D.; Jiang, S.; Zhou, Y.; Du, L., Characterization of the receptor-binding domain (RBD) of 2019 novel coronavirus: implication for development of RBD protein as a viral attachment inhibitor and vaccine. *Cell. Mol. Immunol.* **2020**. DOI: 10.1038/s41423-020-0400-4
- Walls, A. C.; Park, Y. J.; Tortorici, M. A.; Wall, A.; McGuire, A. T.; Velesler, D. Structure, Function, and Antigenicity of the SARS-CoV-2 Spike Glycoprotein. *Cell* **2020**, *181*, 281.
- Tian, X.; Li, C.; Huang, A.; Xia, S.; Shi, Z.; Lu, L.; Jiang, S.; Yang, Z.; Wu, Y.; Ying, T. Potent binding of 2019 novel coronavirus spike protein by a SARS coronavirus-specific human monoclonal antibody. *Emerging Microbes Infect.* **2020**, *9* (1), 382–385.
- Song, W.; Gui, M.; Wang, X.; Xiang, Y. Cryo-EM structure of the SARS coronavirus spike glycoprotein in complex with its host cell receptor ACE2. *PLoS Pathog.* **2018**, *14* (8), No. e1007236.
- Lan, J.; Ge, J.; Yu, J.; Shan, S.; Zhou, H.; Fan, S.; Zhang, Q.; Shi, X.; Wang, Q.; Zhang, L.; Wang, X. Structure of the SARS-CoV-2 spike receptor-binding domain bound to the ACE2 receptor. *Nature* **2020**, *581* (7807), 215–220.
- Brielle, E. S.; Schneidman-Duhovny, D.; Linial, M. The SARS-CoV-2 Exerts a Distinctive Strategy for Interacting with the ACE2 Human Receptor. *Viruses* **2020**, *12* (5), 497.
- He, J.; Tao, H.; Yan, Y.; Huang, S. Y.; Xiao, Y. Molecular Mechanism of Evolution and Human Infection with SARS-CoV-2. *Viruses* **2020**, *12* (4), 428.
- Peng, C.; Zhu, Z.; Shi, Y.; Wang, X.; Mu, K.; Yang, Y.; Zhang, X.; Xu, Z. Exploring the Binding Mechanism and Accessible Angle of SARS-CoV-2 Spike and ACE2 by Molecular Dynamics Simulation and Free Energy Calculation. *ChemRxiv* **2020**.
- Amin, M.; Sorour, M. K.; Kasry, A., Comparing the binding interactions in the receptor binding domains of SARS-CoV-2 and SARS-CoV. *arXiv* **2020**.
- Kollman, P. A.; Massova, I.; Reyes, C.; Kuhn, B.; Huo, S.; Chong, L.; Lee, M.; Lee, T.; Duan, Y.; Wang, W.; Donini, O.; Cieplak, P.; Srinivasan, J.; Case, D. A.; Cheatham, T. E., 3rd Calculating structures and free energies of complex molecules: combining molecular mechanics and continuum models. *Acc. Chem. Res.* **2000**, *33* (12), 889–97.
- Chen, F.; Liu, H.; Sun, H.; Pan, P.; Li, Y.; Li, D.; Hou, T. Assessing the performance of the MM/PBSA and MM/GBSA methods. 6. Capability to predict protein-protein binding free energies and re-rank binding poses generated by protein-protein docking. *Phys. Chem. Chem. Phys.* **2016**, *18* (32), 22129–39.
- Casalino, L.; Palermo, G.; Spinello, A.; Rothlisberger, U.; Magistrato, A. All-atom simulations disentangle the functional dynamics underlying gene maturation in the intron lariet spliceosome. *Proc. Natl. Acad. Sci. U. S. A.* **2018**, *115* (26), 6584–6589.
- Wan, Y.; Shang, J.; Graham, R.; Baric, R. S.; Li, F., Receptor Recognition by the Novel Coronavirus from Wuhan: an Analysis Based on Decade-Long Structural Studies of SARS Coronavirus. *J. Virol.* **2020**, *94* (7). DOI: 10.1128/JVI.00127-20
- Chen, Y.; Guo, Y.; Pan, Y.; Zhao, Z. J. Structure analysis of the receptor binding of 2019-nCoV. *Biochem. Biophys. Res. Commun.* **2020**, *525*, 135.
- Yan, R.; Zhang, Y.; Li, Y.; Xia, L.; Guo, Y.; Zhou, Q. Structural basis for the recognition of SARS-CoV-2 by full-length human ACE2. *Science* **2020**, *367* (6485), 1444–1448.
- Hwang, W. C.; Lin, Y.; Santelli, E.; Sui, J.; Jaroszewski, L.; Stec, B.; Farzan, M.; Marasco, W. A.; Liddington, R. C. Structural basis of neutralization by a human anti-severe acute respiratory syndrome spike protein antibody, 80R. *J. Biol. Chem.* **2006**, *281* (45), 34610–6.
- Prabakaran, P.; Gan, J.; Feng, Y.; Zhu, Z.; Choudhry, V.; Xiao, X.; Ji, X.; Dimitrov, D. S. Structure of severe acute respiratory syndrome coronavirus receptor-binding domain complexed with neutralizing antibody. *J. Biol. Chem.* **2006**, *281* (23), 15829–36.
- Yuan, M.; Wu, N. C.; Zhu, X.; Lee, C. D.; So, R. T. Y.; Lv, H.; Mok, C. K. P.; Wilson, I. A. A highly conserved cryptic epitope in the receptor-binding domains of SARS-CoV-2 and SARS-CoV. *Science* **2020**, *368*, 630.

(29) Zhu, Z.; Chakraborti, S.; He, Y.; Roberts, A.; Sheahan, T.; Xiao, X.; Hensley, L. E.; Prabhakaran, P.; Rockx, B.; Sidorov, I. A.; Corti, D.; Vogel, L.; Feng, Y.; Kim, J. O.; Wang, L. F.; Baric, R.; Lanzavecchia, A.; Curtis, K. M.; Nabel, G. J.; Subbarao, K.; Jiang, S.; Dimitrov, D. S. Potent cross-reactive neutralization of SARS coronavirus isolates by human monoclonal antibodies. *Proc. Natl. Acad. Sci. U. S. A.* **2007**, *104* (29), 12123–8.

(30) Sui, J.; Li, W.; Roberts, A.; Matthews, L. J.; Murakami, A.; Vogel, L.; Wong, S. K.; Subbarao, K.; Farzan, M.; Marasco, W. A. Evaluation of human monoclonal antibody 80R for immunoprophylaxis of severe acute respiratory syndrome by an animal study, epitope mapping, and analysis of spike variants. *J. Virol.* **2005**, *79* (10), 5900–6.

(31) ter Meulen, J.; van den Brink, E. N.; Poon, L. L.; Marissen, W. E.; Leung, C. S.; Cox, F.; Cheung, C. Y.; Bakker, A. Q.; Bogaards, J. A.; van Deventer, E.; Preiser, W.; Doerr, H. W.; Chow, V. T.; de Kruif, J.; Peiris, J. S.; Goudsmit, J. Human monoclonal antibody combination against SARS coronavirus: synergy and coverage of escape mutants. *PLoS Med.* **2006**, *3* (7), No. e237.

(32) Wu, K.; Peng, G.; Wilken, M.; Geraghty, R. J.; Li, F. Mechanisms of host receptor adaptation by severe acute respiratory syndrome coronavirus. *J. Biol. Chem.* **2012**, *287* (12), 8904–11.